Experimental and numerical analysis of three-dimensional semi-rigid steel joints under non-proportional loading

A. Loureiro*, A. Moreno, R. Gutiérrez, J.M. Reinosa

Engineering School, University of A Coruña C/ Mendizabal s/n 15403 Ferrol (Spain)

** Corresponding Author. Tel: +34 981337400 ext 3209, Fax: +34 981337410*

E-mail addresses: loureiro@cdf.udc.es (A. Loureiro), amoreno@cdf.udc.es (A. Moreno)

ruth.gutierrez@udc.es (R. Gutiérrez), jreinosa@udc.es (J.M. Reinosa)

Abstract

This paper focuses on the study of a type of three-dimensional joint that consists of extended end-plates for both major and minor axes. The minor axis connections are bolted to a plate welded to the column flanges (additional plate). An experimental and numerical investigation on the proposed joint is carried out in order to obtain the rotational behaviour (moment–rotation curve) of different three-dimensional configurations, as well as to evaluate the interaction between both axes. Experimental and numerical results show coupling effects between major and minor axis joints. The minor axis load stiffens the tension zone of the mayor axis joint and makes the compression zone more flexible. This leads to a slight increase in the initial stiffness of the major axis joint. The numerical results reveal that the additional plate stiffens the

major axis joint significantly.

Keywords: End-plate connections; Three-dimensional joints; Experimental testing; Finite element modelling; Semi-rigid steel joints.

Link to publisher versión: https://doi.org/10.1016/j.engstruct.2011.12.048
This manuscript version is made available under the CC-BY-NC-ND 4.0 license https://creativecommons.org/licenses/by-nc-nd/4.0/

1. Introduction

Conventional design of steel frameworks is usually carried out under the assumption that joints are either fully rigid or ideally pinned. Modern design codes recognise the concept that the actual joints exhibit a behaviour that is intermediate between these two extreme cases: semi-rigid and nonlinear. AISC-LRFD [1] defines type PR (Partially Restrained) construction, where the effect of joint flexibility must be taken into account in analysis and design procedures. Likewise, Eurocode 3 (EC3) [2] includes procedures and formulations to define both the stiffness and resistance of the semi-rigid joints starting from their geometrical and mechanical properties.

The rotational behaviour of the joint can be described by means of the in-plane moment-rotation curve; this curve defines three main properties: rotational stiffness, moment resistance and rotation capacity. Many studies are aimed at obtaining these moment-rotation curves or the associated properties so that they can be incorporated in the frame analysis. Three main approaches may be followed: experimental, numerical and analytical.

EC3 provides an analytical procedure, called component method, which allows one to evaluate the stiffness and resistance characteristics of the joint by assembling those of all the constitutive components. The principles of the component method are based on works done by Zoetemeijer [3], Yee and Melchers [4] and Jaspart [5]. Faella et al. [6] propose several modifications to this method. In recent years, contributions to this research field have been continuous. Some research studies focus on determining the stiffness and resistance characteristics of the joints [7, 8], while other works focus on obtaining models to calculate the rotation capacity [9-13].

The component method established in the current version of EC3 does not allow the calculation of minor axis joints or three-dimensional joints such as those considered in this paper. Moreover, the formulations do not include the interaction between both axes.

A common design solution for minor axis joints consists of connecting the beam directly to the column web. In such joints, the column web exhibits an out of plane deformation. EC3 only covers the web behaviour loaded in its plane. It is thus necessary to characterize the response of a new component: the column web in transverse bending. Some researchers perform experimental tests and proposals for this component and the subsequent analysis of such joints. The experimental works of Janss et al. [14], Jaspart [5], Gomes et al. [15] and Maquoi [16] show that the column web in bending is responsible for most of the deformation that limits the joint resistance and confirm its typical membrane behaviour.

Cabrero and Bayo [17, 18] propose a new design for three-dimensional joints where the minor axis connections are bolted to a plate welded to the column flanges (additional plate). The additional plate consists of two partial plates in both tension and compression zones. They carry out tests on internal nodes with symmetrical loading. Based on previous theoretical work of Costa Neves et al. [19], they develop an elastic model for the additional plate in bending in both the tension and compression zones.

The advantages of using this type of three-dimensional joint that is characterized by the presence of the additional plate are several. Both major and minor axis connections do not interfere, which makes easier the assembly of the major axis joint. The additional plate acts as a stiffener for the major axis joint and contributes to the resistance of the column web in tension, compression and shear zones. This paper presents the experimental and numerical investigation carried out on this type of three-dimensional joint. The studied joint is shown in Fig. 1. As can be observed, the major and minor axis

connections consist of extended end-plates. The minor axis connections are bolted to an additional plate welded to the column flanges. As seen, the additional plate is executed as a single plate (entire additional plate). The aim is to obtain the rotational behaviour of different three-dimensional configurations, as well as to evaluate the interaction between both axes. In addition, the numerical model, calibrated against tests, allows us to study the effect of the additional plate on the stiffness of the major axis joint.

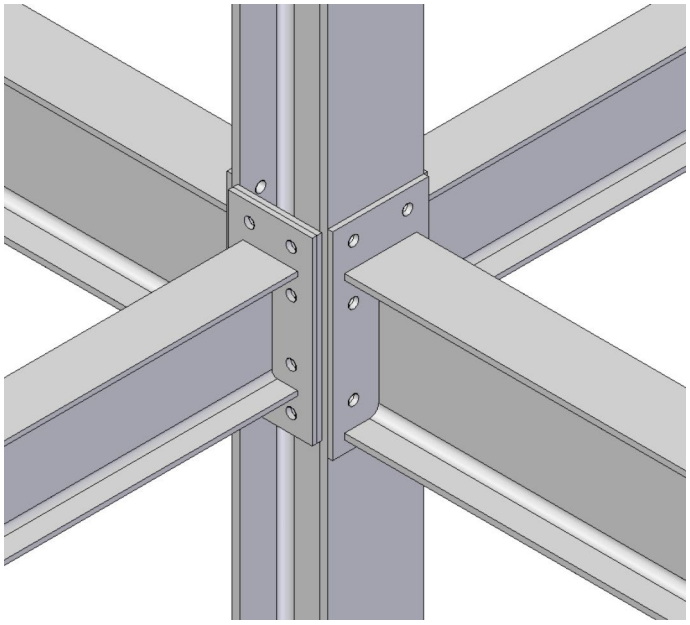


Fig. 1. Proposed three-dimensional semi-rigid joint.

2. Experimental research

2.1. Description of the tests

This experimental investigation comprises four tests on different configurations of the three-dimensional joint proposed in Fig. 1. The geometry of the tested joints is shown in Fig. 2. All the specimens are based on IPE and HEB hot rolled sections. As can be observed, the major axis connections consist of two beams with IPE–240 section connected to a HEB–160 column using an extended end-plate and two tensile bolt rows; the minor axis connections are based on IPE-180 beams connected to the additional plate using a two-side extended end-plate. The plates used are 8 mm thick. TR16 bolts of quality 10.9 in clearance holes are employed. The bolts are designed as bearing type,

category D in EC3; thus, they are hand-tightened up to a torque value of 125 Nm (approximately 30% of that required for preloaded bolts) to ensure the snug-tight condition. The geometry, end-plate thickness and bolts have been chosen to ensure that mode 1 (complete yielding of the end-plate in bending) is the critical mode of failure.

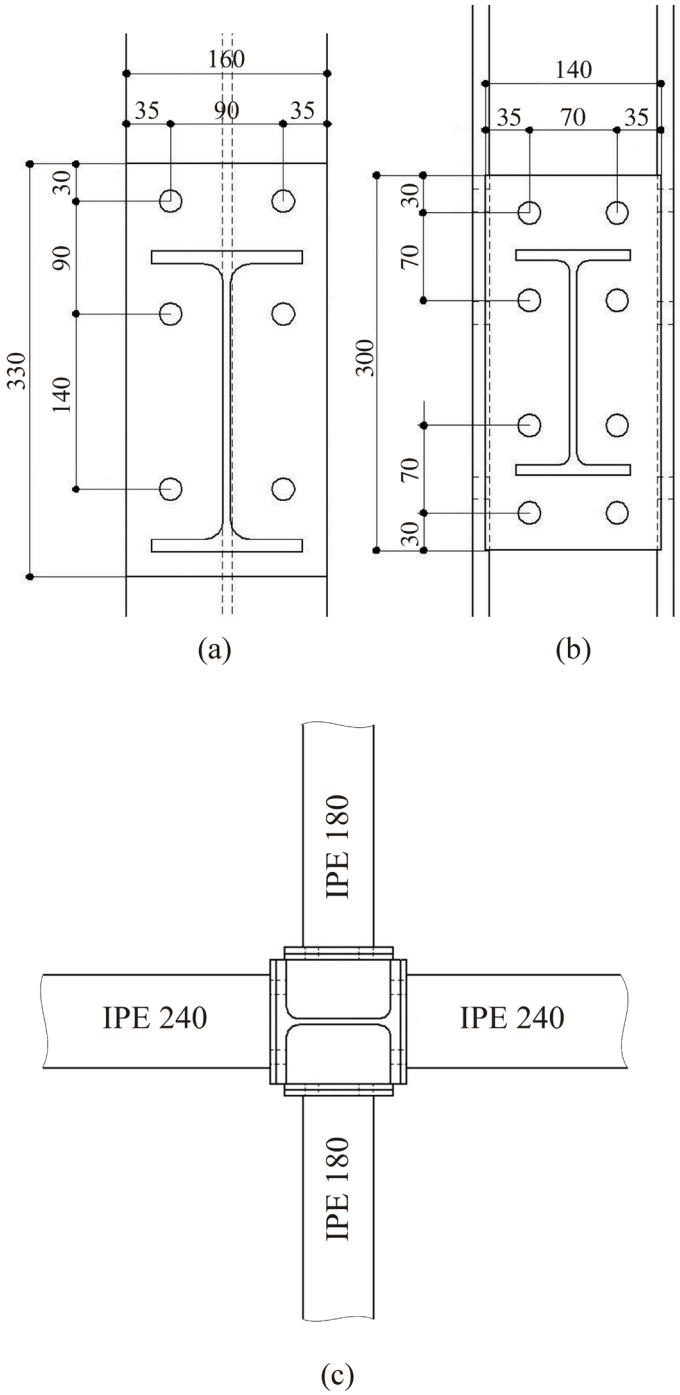


Fig. 2. Geometry of the tested joints. (a) Major axis connection. (b) Minor axis connection. (c) Plan view.

The sections and plates are specified in grade S275 steel. The material properties have been measured in tension tests performed in accordance with UNE-EN 10002-1 [20]. The average properties are set out in Table 1.

The aim of the tests is to obtain the rotational behaviour of different three-dimensional configurations, as well as to assess the interaction between both axes. Three loading configurations are tested (see Fig. 3):

- Internal node with symmetrical loading in the major and minor axes (E01 and E02 tests),
- External joint (E03 test), in which symmetrical loading is applied in the minor axis and a major beam is loaded, and
- Corner joint (E04 test) where a beam of each axis is loaded.

As one can see, in both E03 and E04 tests the non-loaded beams remain arranged in order to make useful measurements. The adopted test setup is shown in Fig. 4(a). The column is fixed supported at both ends and the load is applied to the free end of each beam. The instrumentation comprises load cells, inclinometers, cable-extension displacement sensors (CDS) and strain gauges. These sensors are connected to a System 7000 data acquisition equipment controlled by StrainSmart® software. Details of the instrumentation can be seen in Fig. 4.

Inclinometers are placed in the web of each beam (Fig. 4(b)), at a section close to the joint, and in the column web. The inclinometers placed in the beams measure the absolute rotation of the beams; the one in the column measures the elastic rotation and rigid body motions of the column (superfluous rotations). The rotation of the major axis joints, Φ, is obtained by subtracting these two measurements (Fig. 5): $\Phi = \theta_{\text{INCLI B}} - \theta_{\text{INCLI C}}$.

For bi-dimensional joints; that is, joints without additional plate, the major axis joint rotation includes the web panel shear deformation and the connection rotation. For the three-dimensional joint proposed here, the system formed by the column web and the additional plates, web-plates system, is considered. So, the major axis joint rotation includes the web-plates system shear deformation (E03 and E04) and the connection rotation. The vertical displacement at the end section of the non-loaded beam δ_{CDS2} (see Fig. 5) is measured. This measurement enables the evaluation of the total rotation of the column $\theta_{TOTAL\ C}$ (shear web-plates system deformation plus elastic rotation and rigid body motions of the column). The shear web-plates system deformation, γ, is obtained by subtracting the superfluous rotations from the total rotation of the column: $\gamma = \theta_{TOTAL\ C} - \theta_{INCLI\ C}$.

The employed loading procedure allows us to asses the interaction between the major and minor axis joints; that is, the influence of the minor axis load on the initial stiffness of the major axis joints. A similar loading strategy is used for all tests. Now, it is explained for the tests with symmetrical loading, E01 and E02 (Fig. 3(a)):

Phase 1: bi-dimensional loading. In this phase, the major axis joints are loaded in the elastic range and unloaded afterwards. This loading cycle, comprising both loading and unloading, is repeated twice. This phase of the tests only gives the elastic rotational stiffness of the major axis joints subjected to in-plane loading.

Phase 2: three-dimensional loading. This phase is performed by keeping constant the load acting on the minor axis joints while the load at the end of the major axis beams (Q_M) is increased progressively up to failure. The minor axis joints are loaded up to the onset of their non-elastic behaviour, which corresponds to a moment of 10 kNm. This value is evaluated from the results provided by a numerical model previously developed.

Specimen	Young modulus, E (MPa)	Yield strength, f_y (MPa)	Ultimate strength, f_u (MPa)	Yield strain, ϵ_y (%)	Ultimate strain, ϵ_u (%)
End-plate	222000	277.81	445.12	0.326	10.71
Beam web	208654	348.10	484.80	0.381	36.51
Beam flange	208914	357.83	499.14	0.404	36.76
Column web	208171	301.53	435.84	0.328	35.53
Column flange	206129	315.10	441.12	0.331	35.52

Table 1. Average characteristic values for the structural steel.

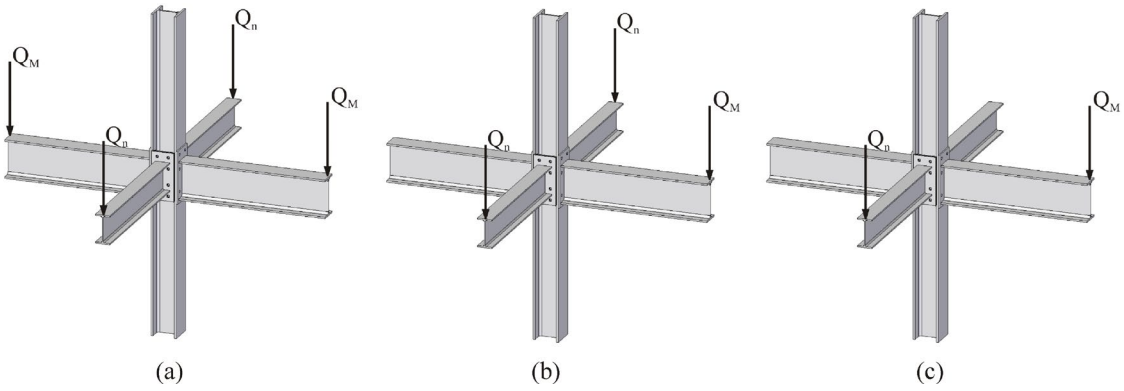


Fig. 3. Tested configurations and loading strategies (three-dimensional loading). (a) Internal joint (E01/E02). (b) External joint (E03). (c) Corner joint (E04).

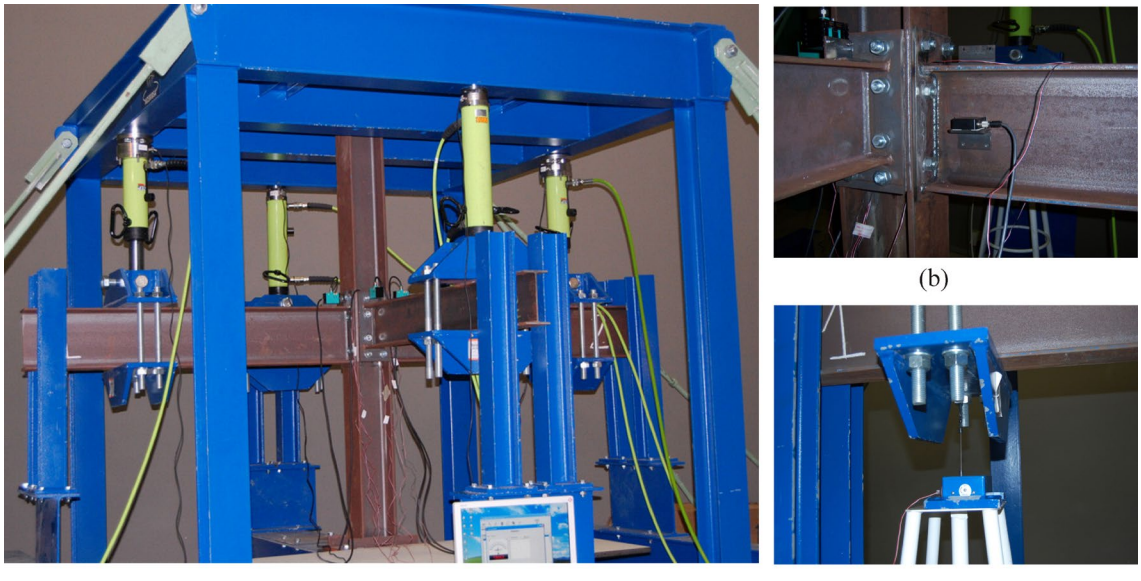


Fig. 4. Test setup and instrumentation. (a) Test setup and load cells (E01 specimen). (b) Inclinometer in the beam (E03). (c) Cable-extension displacement sensor.

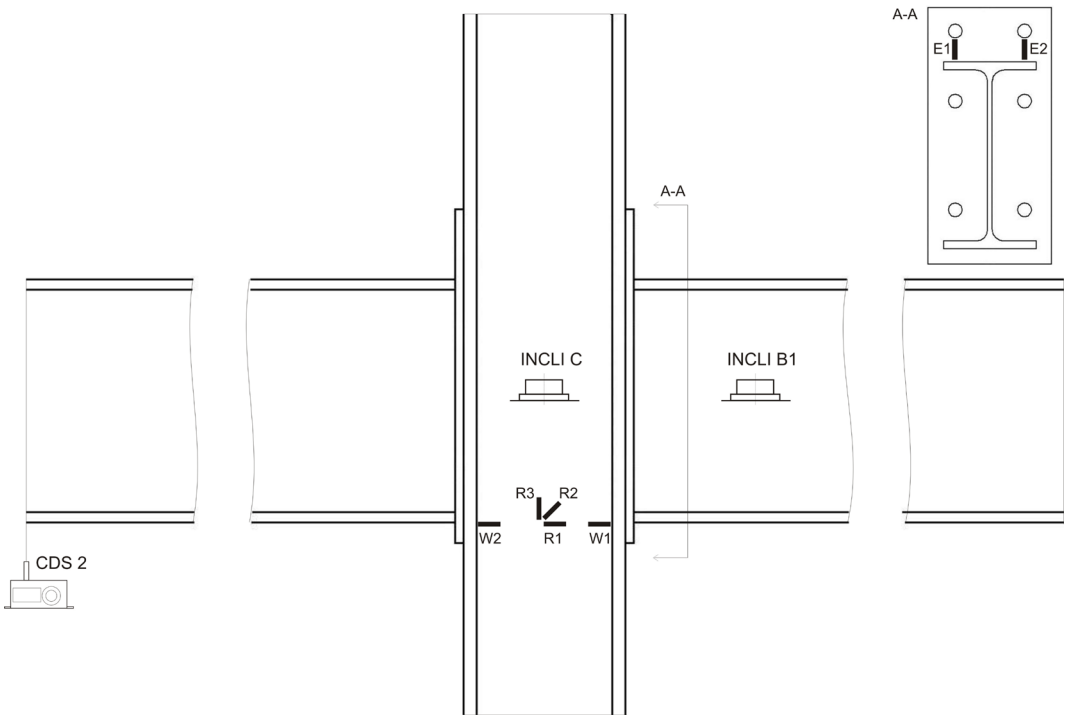


Fig. 5. Major axis instrumentation (E03 and E04 tests).

2.2. Tests results

Fig. 6 shows the moment-rotation curves of the mayor axis joints under three-dimensional loading (phase 2 of the tests). It is observed that the rotational behaviour of the tested joints is characterized by three ranges. A linear range, which is governed by the initial stiffness $S_{j,ini}$, until a moment of $M_{inf,K\text{-}R}$. An intermediate range or transition zone (knee range), up to $M_{sup,K\text{-}R}$; and a final range, whose slope is nearly constant (post-limit stiffness, $S_{j,p\text{-}l}$). All these properties of the curves are given in Table 2. As seen in Fig. 6(c, d), the web-plates system in shear exhibits a high rotational stiffness and a behaviour nearly linear over the entire range of loading.

2.2.1. Discussion of the stiffness results

The initial stiffness values, $S_{j,ini}$, presented here are obtained through linear regression analysis of the quasi-linear branch before the knee region of the curve; the unloading path of the moment-rotation curve corresponding to the second loading cycle is considered [12, 17].

Table 3 shows the initial stiffness values $S_{j,ini}$ of the major axis joints under bi-dimensional loading (2d loading), in comparison with those obtained under three-dimensional loading (3d loading). As is observed, the major axis joints exhibit an increase in the initial stiffness when they are subjected to three-dimensional loading. This increase ranges from 1.7% to 7.6%. This is primarily due to the tensioning effect of the column flanges by the load acting on the minor axis joints.

In E03 and E04 tests, asymmetrical loading in the major axis results in the presence of shear in the joint. In Table 3 it is observed that for both these cases, the shear force causes a reduction in the initial stiffness of the joint compared to E01 and E02 tests.

It is not possible to establish the comparison between the stiffness values obtained from tests and the theoretical values provided by EC3 and the alternative formulation presented in [6], since the components included in EC3 do not take into account the stiffening due to the additional plate or the load acting on the minor axis.

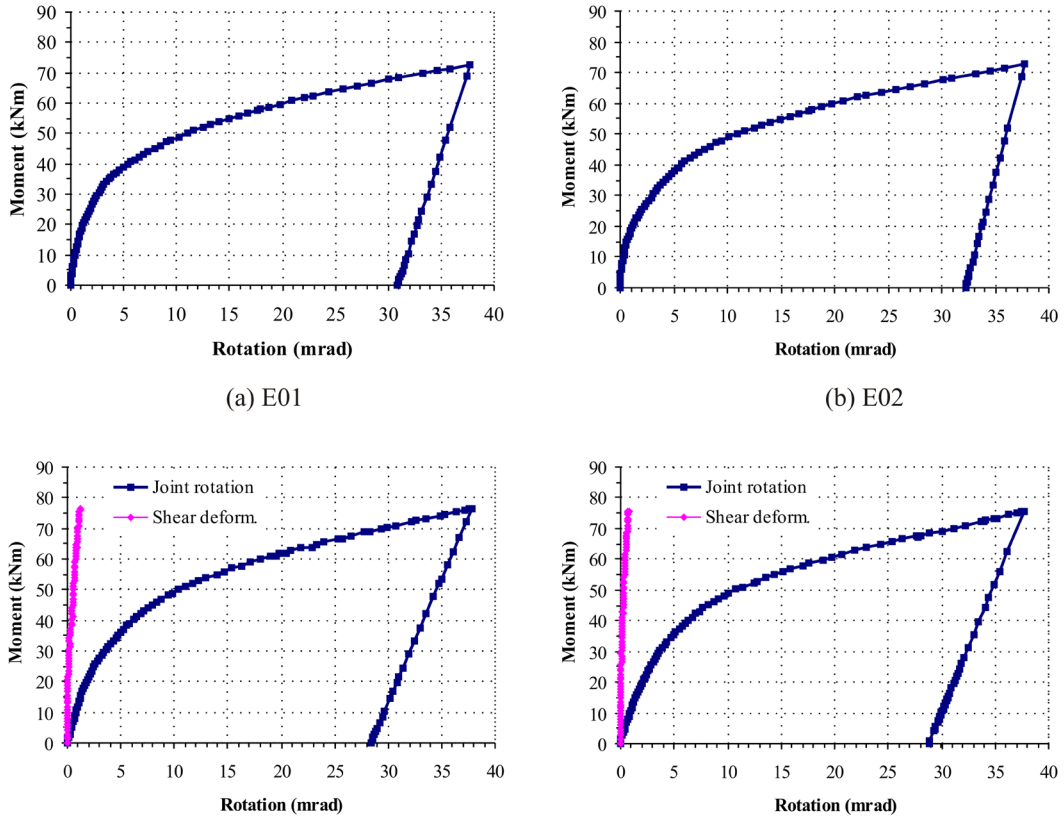
2.2.2. Resistance and mode of failure

While the maximum bending moment, M_{max}, can be identified as the peak resistance of the moment-rotation curve, the moment resistance, $M_{j,Rd}$, is much more difficult to determine accurately. Here the moment resistance, $M_{j,Rd}$, is defined as the intersection point of the two regression lines obtained for the initial and post-limit stiffnesses, as proposed by Zanon and Zandonini [21] and Jaspart [5] and like other authors [12, 17]. Two additional resistance values are also indicated, those corresponding to the beginning, $M_{inf,K-R}$, and end, $M_{sup,K-R}$, of the knee region. All these values are given in Table 2.

Strain gauges are placed at the maximum stress regions of the end-plate and the column web (Fig. 5). The gauges readings (Fig. 7) confirm that the joint failure occurs by complete yielding of the end-plate (mode 1 failure). The end-plate in bending clearly

governs the joint behaviour, being responsible for most of the joint deformation. According to EC3, this mode of failure assures a good ductility of the joint. The gauges located on the column web (Fig. 7) show that all its components remain elastic.

Since the end-plate in bending is not affected by the presence of the additional plate or the minor axis load, we can compare the experimental results with the theoretical results given by EC3 (see Table 4). Considering the definition of the moment resistance $M_{j,Rd}$ proposed in [5, 21] and followed in this paper (approach 1 in Table 4), the EC3 underestimates the joint moment resistance by 35%. The experimental value of the moment resistance $M_{j,Rd}$ also has been determined as the moment corresponding to a secant stiffness equal to 1/3 times the initial one, in accordance with the definition provided by EC3 (approach 2). In this case, the EC3 underestimates the moment resistance about 40%.



(a) E01 (b) E02

(c) E03 (d) E04

Fig. 6. Moment–rotation curves for the tested joints. (a) E01 test. (b) E02 test. (c) E03 test. (d) E04 test.

Test ID	Stiffness (kNm/rad)		Resistance (kNm)			
	$S_{j,ini}$	$S_{j,p-l}$	$M_{inf,K-R}$	$M_{sup,K-R}$	$M_{j,Rd}$	M_{max}
E01	14027.82	747.08	15.80	56.83	47.66	71.24
E02	14985.81	727.61	14.67	57.96	47.47	72.60
E03	11081.80	930.97	14.74	57.12	46.95	76.90
E04	10576.03	873.97	14.85	56.86	47.32	75.64

Table 2. Main characteristics of the moment-rotation curves (3d loading)

Test ID	E01	E02	E03	E04
2d loading	13676.67	13925.77	10534.03	10395.75
3d loading	14027.82	14985.81	11081.80	10576.03
$\Delta S_{j,ini}$ (%)	+2.6%	+7.6%	+5.2%	+1.7%

Table 3. Experimental initial stiffness: comparison for 2d and 3d loading (values in kNm/rad)

In Table 4 it is also observed that EC3 overestimates the moment corresponding to the lower boundary of the knee range, $M_{inf,K-R}$ (30% to 40%).

3. Finite element modelling

A finite element model is developed in Abaqus® [22] in order to predict the rotational behaviour of the studied three-dimensional joint and assess the interaction between both axes.

3.1. Finite element models description

In order to get a simplified model, half of the joint is modelled using symmetry conditions for both internal (E01, E02) and external (E03) joints; in the case of the corner joint (E04), the whole joint is modelled. Linear solid elements with reduced integration and hourglass control (C3D8R) are adopted. In the finite element analyses, the artificial strain energy is very low (approximately 2% of the total internal energy). Details of the finite element meshes are shown in Fig. 8.

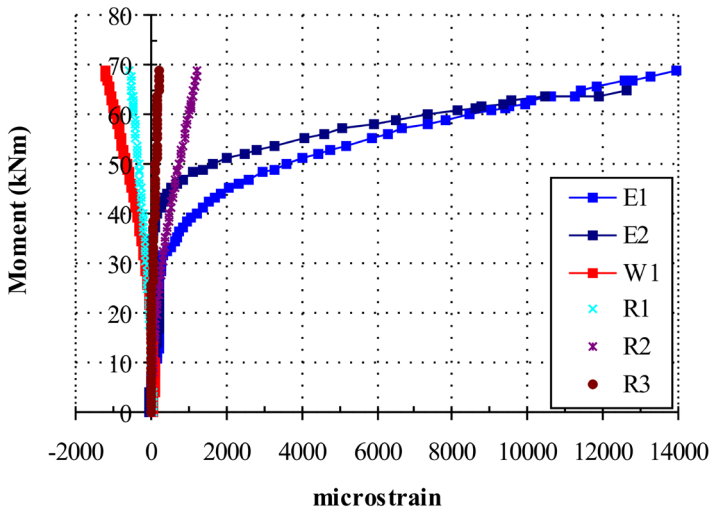
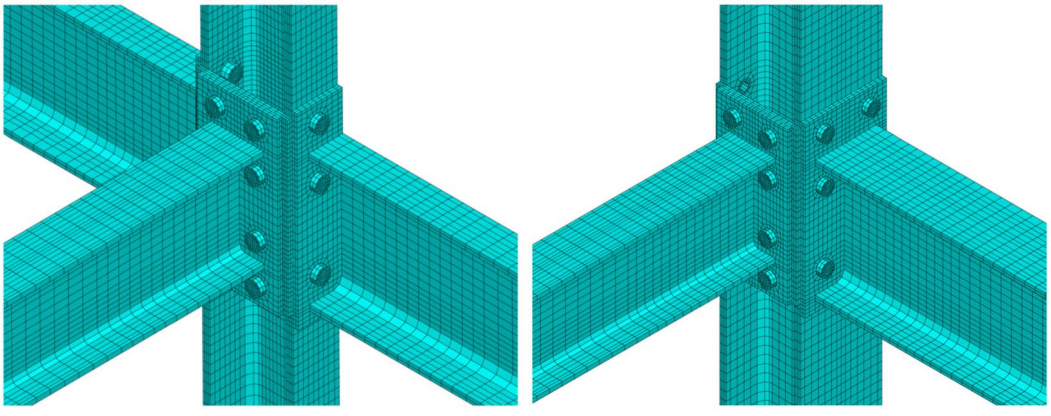


Fig. 7. Moment–strain curves for the external joint (E03 test).

Test ID	$M_{inf,K-R}$			$M_{j,Rd}$				
	EC3	Exp	Ratio EC3/Exp	EC3	Exp approach1	Ratio EC3/Exp	Exp approach2	Ratio EC3/Exp
E01	20.35	15.80	1.29	30.52	47.66	0.64	49.93	0.61
E02	20.35	14.67	1.39	30.52	47.47	0.64	50.94	0.60
E03	20.35	14.74	1.38	30.52	46.95	0.65	52.77	0.58
E04	20.35	14.85	1.37	30.52	47.32	0.64	52.11	0.58

Table 4. Comparison between the experimental and theoretical resistance characteristics (values in kNm).



(a) (b)

Fig. 8: Finite element models. (a) Internal (E01/E02) and external (E03) joints. (b) Corner joint (E04).

Element		Data point	True stress (MPa)	True plastic strain
End-plate		1	278.9	0.0
		2	304.7	0.0140
		3	377.5	0.0319
		4	415.5	0.0487
		5	454.5	0.0697
		6	492.7	0.0994
Beam	web	1	349.4	0.0
	flange	1	358.4	0.0
Column	web	1	302.5	0.0
	flange	1	316.1	0.0
Bolt		1	900	0.0

Table 5. Material plasticity: true stress/strain values provided to Abaqus

A nonlinear static analysis is performed. The analysis includes contact between the components of the joint, considering friction (with a coefficient of 0.25), as well as the effects of geometric nonlinearity and material plasticity. This is defined by means of true stress-strain curves, using the Von Mises yield criteria with isotropic hardening. Table 5 shows the stress-strain data specified in Abaqus to define the material´s plastic behaviour. For the end-plate, a multilinear stress-strain curve defined by six points is employed. For the remaining elements of the joint (beams, column and bolts), the stress-strain curve is taken as perfectly plastic. In the case of the bolts, the nominal value of the yield strength is considered.

3.2. Comparison with experimental results and model validation

Fig. 9 presents the moment-rotation curves of the major axis joints under three-dimensional loading resulting from the numerical analyses along with those of the corresponding tests. The comparison shows that the proposed model closely reproduces the joint behaviour over the entire range of loading.

The numerical model is also validated by comparing the true strain results (LE) from the simulation with the gauges readings. Fig. 10 shows this comparison for the external

joint (E03). As can be observed, the moment-strain curves predicted by the analysis are in excellent agreement with those obtained from test.

The final deformed shape of the internal joint (E01/E02) is shown in Fig. 11, along with the deformed joint for the E01 test. Fig. 12 shows the stress distribution, corresponding to the beginning of the knee range ($M_{\text{inf,K-R}}$), for the corner joint (E04).

Table 6 shows the initial stiffness values $S_{\text{j,ini}}$ of the major axis joints for both bi-dimensional (2d loading) and three-dimensional loading (3d loading). As is observed, the increase in stiffness is very small. However, coupling effects in the column flange have been observed in both the tests and the numerical analyses. The numerical model presented here allows us to study these effects not only in the column flange, but also in the rest of components affected by the minor axis load, as will be seen in Section 4.2.

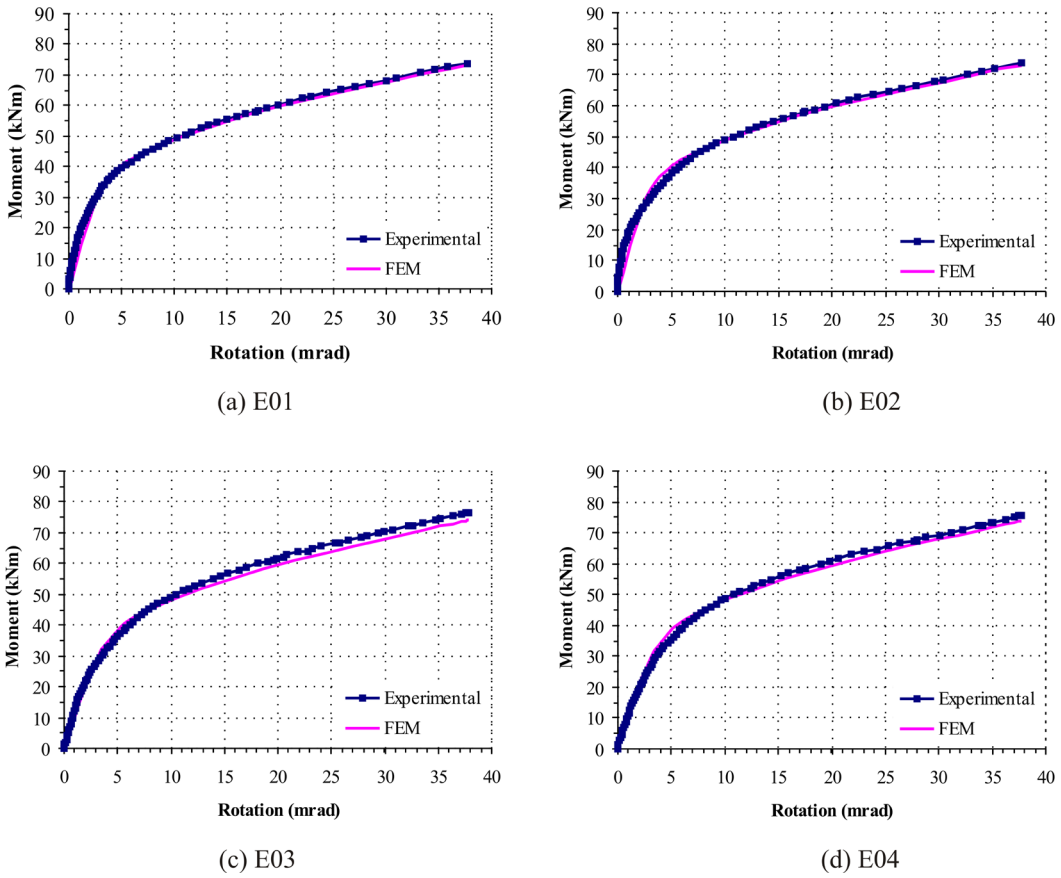


Fig. 9. Numerical and experimental moment–rotation curves. (a) E01 test. (b) E02 test. (c) E03 test. (d) E04 test.

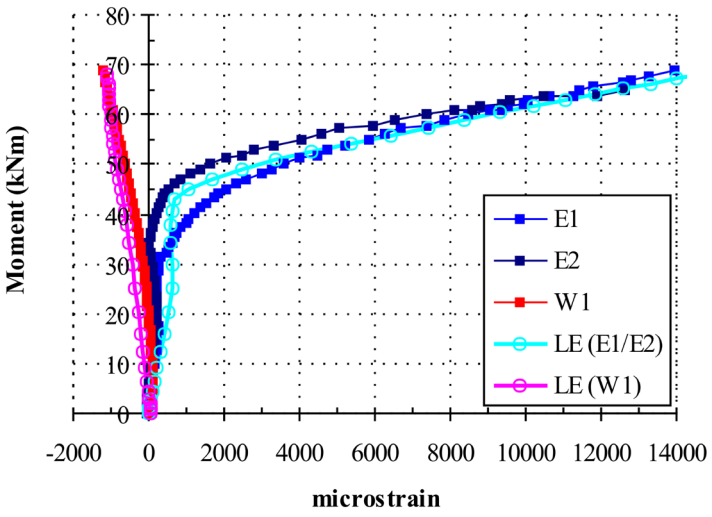
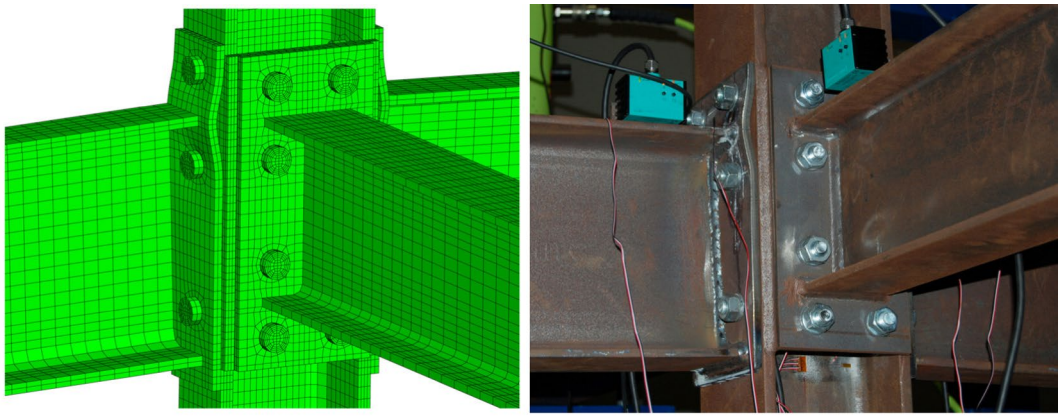


Fig. 10. Experimental and numerical moment-strain curves for the external joint (E03 test).



(a) (b)

Fig. 11. Deformed shape of the internal joint. (a) Finite element model (E01/E02). (b) Test (E01).

4. Elastic behaviour of the proposed three-dimensional joint

The validated numerical model allows us to study the effect of the additional plate welded to the column flanges and the three-dimensional loading on the initial stiffness of the major axis joint.

4.1. Effect of the additional plate

Due to the additional plate, the increase in stiffness is of 17% and 25% for symmetrical (E01/E02) and asymmetrical loading (E03/E04), respectively.

According to the component method suggested by EC3, the rotational stiffness of the joint is obtained from the axial deformations Δ_i of the components in the force paths:

$$S_{\mathrm{j,ini}} = \frac{M}{\Phi} = \frac{Fz}{\frac{\sum \Delta_i}{z}} = \frac{Fz^2}{\sum \Delta_i} \quad (1)$$

where z is the equivalent lever arm. Here the axial deformations of the components of the joint without additional plate (2D joint) are compared with those of the joint with additional plate under bi-dimensional loading (3D-q2 joint). The following components are considered: column flange in bending (cfb), column web in tension (cwt), compression (cwc) and shear (cws), and additional plate in tension (apt), compression (apc) and shear (aps).

Table 7 shows the deformation values Δ_i of the components for symmetrical (E01/E02) and asymmetrical loading (E03/E04). The deformation values (in millimetres) correspond to the beginning of the knee range ($M_{\mathrm{inf,K\text{-}R}}$).

4.1.1. Column flange in bending

As is observed from the results of Table 7, the stiffness of the column flange in bending (cfb) increases up to approximately double due to the additional plate. The reason is that the additional plate changes the behavior of T-stub representing the column flange bending; this goes from a cantilever beam (Fig. 13) to a beam in which the degree of restraint between the column flange in bending and the additional plate in tension depends on the relative stiffness of both components (Fig. 14).

4.1.2. Column web

The results of Table 7 also show that the deformations of the column web in tension (cwt), compression (cwc) and shear (cws) of the joint with additional plate (3D-q2) decrease between 20% and 30%; this indicates that tensile, compressive and shear forces distribute between the column web and the additional plates.

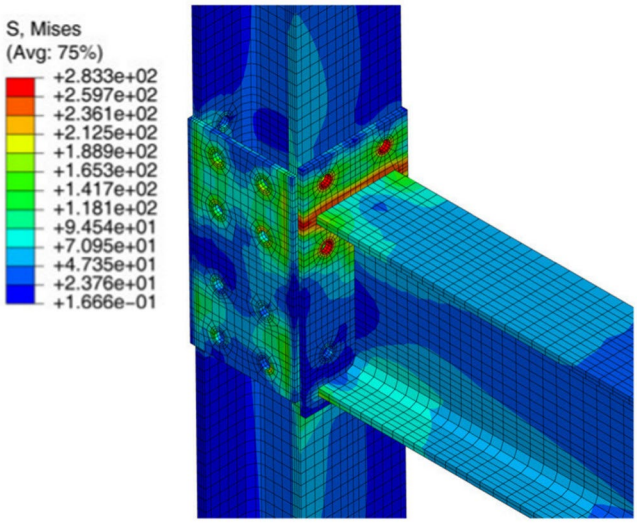


Fig. 12: Stress distribution (in MPa) for the corner joint (E04).

Test ID	EF (E01/E02)	EF (E03)	EF (E04)
2d loading	12112.25	10178.73	10178.73
3d loading	12366.61	10337.65	10270.34
$\Delta S_{j,ini}$ (%)	+2.1%	+1.6%	+0.9%

Table 6. Numerical initial stiffness: comparison for 2d and 3d loading (values in kNm/rad).

Test ID		E01/E02		E03/E04	
		2D	3D-q2	2D	3D-q2
Bolt-row 1	cfb	0.0687	0.0318	0.0667	0.0316
	cwt	0.0122	0.0090	0.0118	0.0090
	apt	-	0.0039	-	0.0040
	cw-ap	-	0.0063	-	0.0063
Bolt-row 2	cfb	0.0798	0.0391	0.0758	0.0378
	cwt	0.0172	0.0129	0.0162	0.0129
	apt	-	0.0044	-	0.0045
	cw-ap	-	0.0083	-	0.0084
Compression	cwc	0.0371	0.0305	0.0359	0.0285
	apc	-	0.0110	-	0.0137
	cw-ap	-	0.0201	-	0.0206
Shear	cws	-	-	0.1048	0.0707
	aps	-	-	-	0.0245
	cw-ap	-	-	-	0.0547

Table 7. Effect of the additional plate: deformation of the components of the 2D joint and 3D-q2 joint (values in millimetres).

In order to compare stiffness values, the system formed by the column web and the additional plates (web-plates system) in tension, compression and shear is considered. The stiffness values of the web-plates system (cw-ap) relative to those of the column web of the joint without additional plate, $k_{cw\text{-}ap} / k_{cw}$, have been calculated. The values of $k_{cw\text{-}ap} / k_{cw}$ are 2.0 and 1.8 for the tension and compression zones, respectively. A value of $k_{cw\text{-}ap} / k_{cw} = 1.9$ is obtained for the shear zone.

It is observed that the $k_{cw\text{-}ap} / k_{cw}$ ratio in the tension zone is greater than that of the compression zone. This is due to the length of the additional plate in the compression zone. It has been found that extending the additional plate throughout the effective width of the web in compression (see Fig. 15), the stiffness of the web-plates system increases such that $k_{cw\text{-}ap} / k_{cw} = 2.0$.

4.1.3. Comparison with theoretical results

In order to compare the stiffness values obtained from tests with those predicted by the component method, the formulas provided by EC3 and Faella at el. [6] are modified to include the stiffening due to the additional plate. These modifications are made in accordance with the numerical results just presented. To take into account the effect of the additional plate on the stiffness of the column flange in bending, the stiffness coefficient proposed by EC3 and Faella et al. [6] is multiplied by 2.0. In the case of the web-plates system, the stiffness coefficients provided by the EC3 and Faella et al. [6] for the column web in tension, compression and shear are multiplied by 2.0, 1.8 and 1.9, respectively. The formulas corresponding to the end-plate in bending and bolts in tension are not modified, since these components are not affected by the additional plate.

Table 8 shows the experimental results corresponding to the joint with additional plate under bi-dimensional loading (3D-q2), along with those obtained by modifying the

formulas described in EC3 and [6]. The best agreement with the experimental results is obtained by applying the formulation proposed by Faella et al. [6]. As is observed, this underestimates the stiffness from 5% to 8%; on the contrary, the formulation in EC3 leads to an overestimation of the stiffness from 20% to 30%.

4.2. Effect of the three-dimensional loading (minor axis load)

Here we study the influence of the minor axis load on the elastic response of the components of the major axis joint.

The column flange in bending and the additional plate in tension and compression are the components that exhibit more variation in their behavior under three-dimensional loading. Table 9 shows the deformation values Δ_i of these components for both bi-dimensional (3D-q2) and three-dimensional loading (3D-q3). The effect of the minor axis load on the components of the column web (in tension, compression and shear), as well as on the additional plate in shear is not significant, so they are not showed in Table 9.

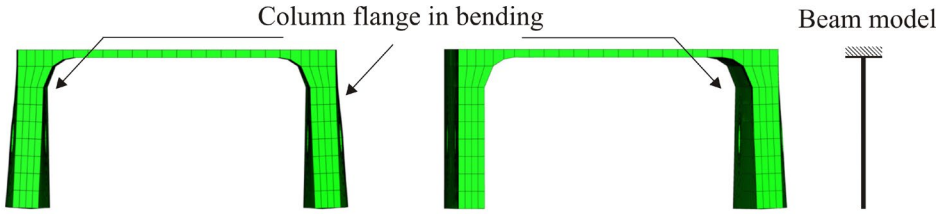


Fig. 13. Deformed shape of the column flange in bending: joint without additional plate. (a) Symmetrical loading (E01/E02). (b) Asymmetrical loading (E03/E04).

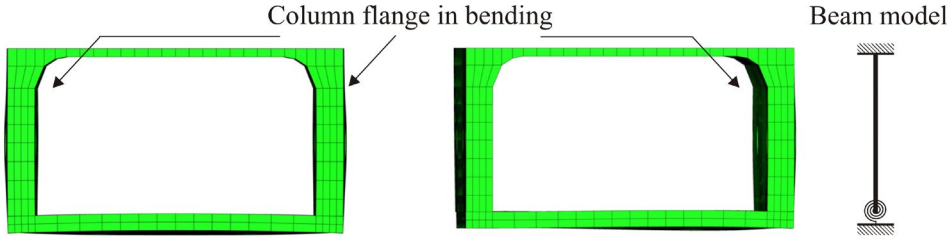


Fig. 14. Deformed shape of the column flange in bending: joint with additional plate. (a) Symmetrical loading (E01/E02). (b) Asymmetrical loading (E03/E04).

4.2.1. Tension zone

As is observed from the results of Table 9, the column flange in bending (cfb) and the additional plate in tension (apt) show an increase in stiffness of 5% and 8%, respectively, under three-dimensional loading (3D-q3). Fig. 16 illustrates the influence of the minor axis load on the deformation of these components for the corner joint (E04). The tensile force arising from the moment applied on the minor axis joint $F_{b,n}$ produces a tensile axial force in the column flange, thus decreasing its deformation in bending Δ_{cfb}. In the case of the additional plate, the force corresponding to the minor axis moment $F_{b,n}$ causes a reduction in the axial deformation of the additional plate Δ_{apt}. The effect of bending plus tensile axial force on these two components is favorable, since it results in an increase in the stiffness.

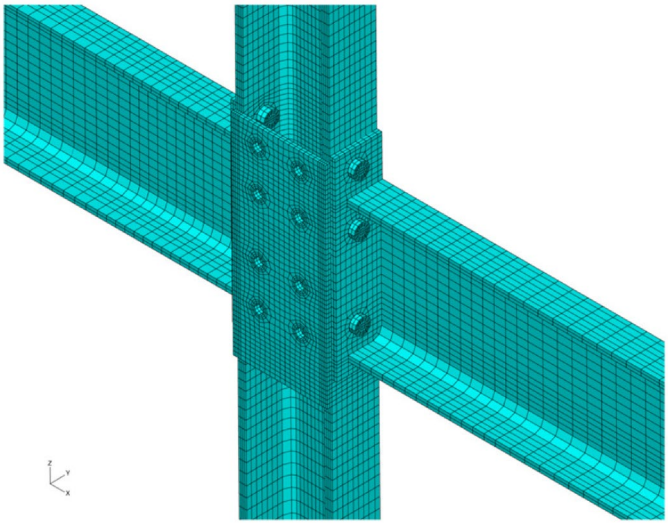


Fig. 15. Model with end-plate extended throughout the effective width of the web in compression.

4.2.2. Compression zone

The results of Table 9 also show that the additional plate in compression (apc) becomes more flexible under three-dimensional loading (3D-q3). In this case, the force associated with the minor axis moment $F_{b,n}$ produces an increase in the axial

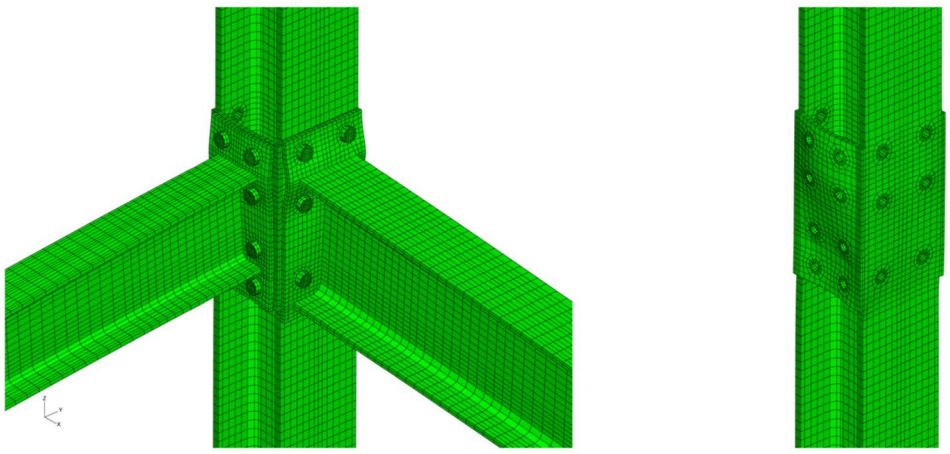
deformation of the additional plate Δ_{apc} (see Fig. 16). Now, the effect of minor axis bending plus compression axial force is unfavorable, decreasing the stiffness of this component by 10%.

Test ID	E01	E02	E03	E04
Experimental	13676.67	13925.77	10534.03	10395.75
EC3 $_{modified}$	16885.85	16885.85	13217.41	13217.41
	+23.5%	+21.2%	+25.5%	+27.1%
Faella $_{modified}$	12809.52	12809.52	9864.09	9864.09
	−6.3%	−8.0%	−6.3%	−5.1%

Table 8. Comparison between the experimental and theoretical initial stiffness values (in kNm/rad).

Test ID		E01/E02		E03		E04	
		3D-q2	3D-q3	3D-q2	3D-q3	3D-q2	3D-q3
Bolt-row 1	cfb	0.0318	0.0303	0.0316	0.0306	0.0316	0.0309
	apt	0.0039	0.0037	0.0040	0.0037	0.0040	0.0039
Bolt-row 2	cfb	0.0391	0.0373	0.0378	0.0366	0.0378	0.0369
	apt	0.0044	0.0040	0.0045	0.0040	0.0045	0.0042
Compression	apc	0.0110	0.8953	0.0137	0.0153	0.0137	0.0145

Table 9. Effect of the three-dimensional loading: deformation of the components of the 3D-q2 joint and 3D-q3 joint (values in millimetres).



(a) (b)

Fig. 16. Effect of the three-dimensional loading: corner joint (E04). (a) Whole joint. (b) Column side.

5. Conclusions and further research

- This paper focuses on the study of a type of three-dimensional node with semi-rigid joints in both axes. The major and minor axis connections consist of extended end-plates because of their cost effectiveness and the ease with which they can be produced and assembled.
- The proposed joint has been studied by means of experimental tests in order to obtain the rotational behaviour of different three-dimensional configurations, as well as to assess the interaction between both axes; that is, the effect of the minor axis load on the initial stiffness of the major axis joint.
- The theoretical values of the moment resistance of the joint $M_{j,Rd}$ have been compared with the experimental ones obtained by applying different definitions. For the joints studied in this work, the results show that the EC3 underestimates the moment resistance by 35% (for Zanon and Zandonini [21] and Jaspart [5] definition) and about 40% (for the definition according to EC3); and however, the EC3 overestimates the moment corresponding to the lower boundary of the knee range, $M_{inf,K\text{-}R}$ (30% to 40%).
- The numerical model calibrated against tests allows us to evaluate the influence of the minor axis load and the additional plate on the elastic behaviour of the components of the major axis joint, and so, on the initial stiffness of the joint.
- Experimental and numerical results show coupling effects between the major and minor axis joints. The minor axis load stiffens the column flange in bending and the additional plate in tension, and makes the additional plate in compression more flexible. This results in a slight increase in the initial stiffness of the major axis joint.
- The numerical results reveal that the additional plate has a significant influence on the stiffness of the major axis joint. The additional plate stiffens the column flange

and the system formed by the column web and the additional plates in the tension, compression and shear zones of the joint. In addition, it has been observed that the extension of the additional plate throughout the tension and compression zones influences the behavior of the major axis joint, thus being a parameter to consider in the three-dimensional joint design.

- In order to compare the stiffness values obtained from tests with those predicted by the component method, the formulas provided by EC3 and Faella at el. [6] are modified to include the stiffening due to the additional plate, taking into account the numerical results.
- The validated numerical model will allow us to carry out parametric studies in order to assess the interaction between both axes in terms of stiffness and resistance for geometries and levels of minor axis load different from those considered in this study.
- Further research is needed to obtain the initial stiffness of the major axis joints of the proposed three-dimensional node by means of the component method. The aim is to modify the formulations provided by EC3 and Faella et al. [6] in order to include the stiffening due to the additional plate. The components to be investigated are: the column flange in bending and the system formed by the column web and the additional plates in tension, compression and shear, as seen in the course of this investigation.

Acknowledgments

The authors would like to thank the Spanish Ministry of Science and Innovation for the financial assistance of this work by means of the project “Analysis and global design of three-dimensional semi-rigid steel joints under conditions of asymmetric loads and form”, BIA2010-20839-C02-01.

References

[1] LRFD. Load and resistance factor design: manual of steel construction. 3rd ed. American Institute of Steel Construction; 2003.

[2] CEN, Eurocode 3: Design of steel structures. Part 1.8: Design of Joints (EN 1993-1-8). 2005.

[3] Zoetemeijer P. Summary of the research on bolted beam-to-column connections (period 1978-1983). Tech. rep. 6-85-M. Delft: Steven Laboratory; 1983.

[4] Yee YL, Melchers RE. Moment–Rotation curves for bolted connections. Journal of Structural Engineering ASCE 1986; 112(3): 615–35.

[5] Jaspart JP. Etude de la semi-rigidité des noeuds poutre-colonne et son influence sur la resistance et la stabilité des ossatures in acier. PhD thesis. University of Liège, Liège; 1991.

[6] Faella C, Piluso V, Rizzano G. Structural steel semirigid conections: Theory, design and software. In: New directions in civil engineering. Boca Raton (Florida): CRC Publishers; 2000.

[7] Loureiro A, Gutiérrez R, Reinosa JM, Moreno A. Axial stiffness prediction of non-preloaded T-Stubs: An analytical frame approach. Journal of Constructional Steel Research 2010; 66: 1516-22.

[8] Loureiro A, Reinosa JM, Gutiérrez R, Moreno A. New proposals on the calculation of the flexural resistance in angle connections. Journal of Constructional Steel Research 2011; 67: 613-22.

[9] Faella C, Piluso V, Rizzano G. Plastic deformation capacity of bolted T-stubs. International workshop and seminar on behaviour of steel structures in seismic areas, STESSA ´97. Kyoto (Japan); 1997.

[10] Faella C, Piluso V, Rizzano G. Prediction of bolted connection ductility. International workshop and seminar on behaviour of steel structures in seismic areas, STESSA ´97. Kyoto (Japan); 1997.

[11] da Silva LS, Santiago A, Real PV. Post-limit stiffness and ductility of end-plate beam-to-column steel joints. Computers and Structures 2002; 80: 515-31.

[12] Girão Coelho AM, Bijlaard FSK, da Silva LS. Experimental assessment of the ductility of extended end plate connections. Engineering Structures 2004; 26: 1185-206.

[13] Gil B, Cabrero JM, Goñi R, Bayo E. An assessment of the rotation capacity required by structural hollow sections for plastic analysis. In: Jaurrieta MA, Alonso A, Chica JA, editors. Tubular structures X. Lisse (Holland): A.A. Balkema Publishers; 2003, p. 277-92.

[14] Janss J, Jaspart JP, Maquoi R. Strength and behaviour of in plane weak axis joints and 3D joints. In: Proc. of the state of the art workshop on connections and the behaviour, strength and design of steel structures; 1987, p. 60-8.

[15] Gomes FCT, Jaspart JP, Maquoi R. Moment capacity of beam-to-column minor axis joints. In: Proceedings of the IABSE international colloquium on semi-rigid structural connections. Istambul (Turkey): IABSE; 1996, p. 319-26.

[16] Maquoi R, Jaspart JP, Guisse S, Lognard B, Taquet F. Etude expérimentale et théorique du comportement des noeuds poutre-colonne d´axe faible. Sixième rapport semestriel. Recherche COST C1 Région Wallonne – Université de Liège ; 1995.

[17] Cabrero JM, Bayo E. The semi-rigid behaviour of the three-dimensional steel beam-to-column joints subjected to proportional loading. Part I: Experimental evaluation. Journal of Constructional Steel Research 2006; 63: 1241-53.

[18] Cabrero JM, Bayo E. The semi-rigid behaviour of the three-dimensional steel beam-to-column joints subjected to proportional loading. Part II: Theoretical model and validation. Journal of Constructional Steel Research 2006; 63: 1254-67.

[19] Costa Neves L, da Silva LS, Vellasco P. A model for predicting the stiffness of beam to concrete filled column and minor axis joints under static monotonic loading. In: Hoffmeister B, Hechler O, editors. Eurosteel 2005 – 4th European conference on steel and composite structures, vol. C. Maastricht: Verlag Mainz; 2005. p. 4.10-131 – 4.10-138.

[20] UNE-EN 10002-1: Materiales metálicos. Ensayos a tracción. Parte 1: Método de ensayo a temperatura ambiente. AENOR; 2002.

[21] Zanon P, Zandonini R. Experimental analysis of end plate connections. In: Proc. of the state of the art workshop on connections and the behaviour, strength and design of steel structures; 1988, p. 41-51.

[22] ABAQUS User´ Manual. Version 6.7. USA: Hibbit, Karlsson & Sorensen, Inc.; 2007.